

Centrality and pseudorapidity dependence of elliptic flow for charged hadrons in  
Au+Au collisions at  $\sqrt{s_{NN}} = 200$  GeV

B B Back<sup>1</sup>, M D Baker<sup>2</sup>, M Ballintijn<sup>4</sup>, D S Barton<sup>2</sup>, R R Betts<sup>6</sup>, A A Bickley<sup>7</sup>, R Bindel<sup>7</sup>, A Budzanowski<sup>3</sup>,  
W Busza<sup>4</sup>, A C Carroll<sup>2</sup>, M P Decowski<sup>4</sup>, E Garcia<sup>6</sup>, N K George<sup>1,2</sup>, K Gulbrandsen<sup>4</sup>, S Gushue<sup>2</sup>,  
C Halliwell<sup>6</sup>, J Hamblen<sup>8</sup>, G A Heintzelman<sup>2</sup>, C Henderson<sup>4</sup>, D Hofman<sup>6</sup>, R S Hollis<sup>6</sup>, R Holynski<sup>3</sup>,  
B Holzman<sup>2</sup>, A Jordanova<sup>6</sup>, E Johnson<sup>8</sup>, J L Kane<sup>4</sup>, J Katz<sup>4,6</sup>, N Khan<sup>8</sup>, W Kuczewicz<sup>6</sup>, P Kulinchik<sup>4</sup>,  
C M Ku<sup>5</sup>, W T Lin<sup>5</sup>, S Manly<sup>8</sup>, D M McLeod<sup>6</sup>, A C Mignerey<sup>7</sup>, M Nguyen<sup>2</sup>, R Nouicer<sup>6</sup>, A Olszewski<sup>3</sup>,  
R Pak<sup>2</sup>, I C Park<sup>8</sup>, H Pemegger<sup>4</sup>, C Reed<sup>4</sup>, L P Remsberg<sup>2</sup>, M Reuter<sup>6</sup>, C Roland<sup>4</sup>, G Roland<sup>4</sup>,  
L Rosenberg<sup>4</sup>, J Sagerer<sup>6</sup>, P Sarin<sup>4</sup>, P Sawicki<sup>8</sup>, W Skulski<sup>8</sup>, P Steinberg<sup>2</sup>, G S F Stephanus<sup>4</sup>,  
A Sukhanov<sup>2</sup>, J L Tang<sup>5</sup>, M B Tonjes<sup>7</sup>, A Trzupek<sup>3</sup>, C M Vale<sup>4</sup>, G J van Nieuwenhuizen<sup>4</sup>,  
R Verdier<sup>4</sup>, G Vlachos<sup>4</sup>, F L H Wolfs<sup>8</sup>, B Wosiek<sup>3</sup>, K Wozniak<sup>3</sup>, A H Wuosmaa<sup>1</sup>, B Wyslouch<sup>4</sup>

<sup>1</sup> Argonne National Laboratory, Argonne, IL 60439-4843, USA

<sup>2</sup> Brookhaven National Laboratory, Upton, NY 11973-5000, USA

<sup>3</sup> Institute of Nuclear Physics PAN, Krakow, Poland

<sup>4</sup> Massachusetts Institute of Technology, Cambridge, MA 02139-4307, USA

<sup>5</sup> National Central University, Chung-Li, Taiwan

<sup>6</sup> University of Illinois at Chicago, Chicago, IL 60607-7059, USA

<sup>7</sup> University of Maryland, College Park, MD 20742, USA

<sup>8</sup> University of Rochester, Rochester, NY 14627, USA

(Dated: 12th July, 2004)

This paper describes the measurement of elliptic flow for charged particles in Au+Au collisions at  $\sqrt{s_{NN}} = 200$  GeV using the PHOBOS detector at the Relativistic Heavy Ion Collider (RHIC). The measured azimuthal anisotropy is presented over a wide range of pseudorapidity for three broad collision centrality classes for the first time at this energy. Two distinct methods of extracting the flow signal were used in order to reduce systematic uncertainties. The elliptic flow falls sharply with increasing  $\eta$  at 200 GeV for all the centralities studied, as observed from minimum-bias collisions at  $\sqrt{s_{NN}} = 130$  GeV.

PACS numbers: 25.75.-q

It is widely accepted that a very dense and possibly new state of matter is being created in central Au+Au collisions [1] at the Relativistic Heavy-Ion Collider (RHIC) at Brookhaven National Laboratory. The dynamical evolution of such collisions is of great interest. The azimuthal anisotropies of the number of produced particles ("flow") result from the initial spatial asymmetry of the collision zone and subsequent rescattering processes, which convert the initial spatial anisotropy into azimuthal anisotropy. Therefore, measurements of the particle flow state azimuthal anisotropy provide a useful tool to probe both the conditions prevailing in an early stage of the collision system and the dynamical evolution of the system.

There is an extensive data set on flow results from RHIC [2, 3, 4, 5, 6, 7, 8, 9, 10, 11, 12], but as of yet the least understood result is the pseudorapidity and energy dependence of the elliptic flow,  $v_2(\eta)$ , measured over an extended  $\eta$ -range [11, 12]. Current models are unable to simultaneously reproduce the shape of the charged particle pseudorapidity density ( $dN/d\eta$ ) and the  $v_2(\eta)$  dependence. In this paper we examine the dependence of the  $v_2(\eta)$  shape on the collision centrality. The elliptic flow of charged hadrons has been studied using data from the PHOBOS detector during the 2001 Au+Au run of RHIC. In addition to the "hit-based"

method previously used in [11], a new "track-based" method was developed and employed to improve the accuracy of the measurement and provide a valuable consistency check of the hit-based analysis.

The PHOBOS detector consists of silicon pad detectors arranged in single and multiple-layer configurations surrounding the interaction region as described in [13]. The multiple-layer configurations are used to find tracks over a specific pseudorapidity and azimuthal region. These detectors include the vertex detector (VTX) ( $|\eta| < 0.92$ ,  $= 43^\circ$ ) and the two magnetic spectrometer tracking arms (SPECP and SPENC) ( $0 < |\eta| < 1.8$ , each arm subtending  $= 22^\circ$  centered at  $= 0^\circ$  and  $180^\circ$  for tracks traversing the field free region). Each spectrometer arm is configured such that there is a tracking region prior to the magnetic field and another in the field. Therefore, two distinct classes of tracks are found, "straight-line" tracks ( $0.0 < |\eta| < 1.8$ ) with no momentum measurement and "curved" tracks ( $0.0 < |\eta| < 1.5$ ) with momentum measurement. Details of the tracking procedure are given elsewhere [14]. The single layer configuration is used to achieve large pseudorapidity coverage, where particles are detected from energy depositions in the silicon pads. These detectors include the octagonal multiplicity detector (OCT) ( $|\eta| < 3.2$ ) and six annular silicon ring multiplicity detectors ( $3.0 < |\eta| < 5.4$ ). The

rings and most of the octagon have complete 2<sup>o</sup> coverage in azimuth, except for octagon openings around the nominal interaction position. These openings are for tracks that go through to the multiple-layer detectors of the VTX and SPECN and SPECP detectors.

Two sets of scintillating paddle counters were used for triggering and centrality determination as described in [15, 16]. In addition an online vertex trigger was employed, using two sets of Cerenkov detectors. The hit-based method requires events whose collision vertex ( $v_z$ ) is centered at 34 cm away from the nominal vertex position, along the beam axis [11]. The vertex trigger enabled a special high statistics sample ( 1 million triggers) of such events to be taken. The track-based method required events with vertices within about 10 cm of the nominal vertex position, which allowed a large fraction of the 2001 Au+Au data set at 200 GeV ( 25 million triggers) to be used with this method. The minimum-bias sample for the hit-based method consists of all triggered events that have a valid reconstructed vertex. This engenders biases similar to those discussed in [11] and leads to the average number of participants ( $\langle N_{\text{part}} \rangle$ ) given in Table I. For the track-based method only the fraction of the cross-section unbiased by trigger and vertex inefficiencies is used to form the minimum-biased sample. The average number of participants for this method is also given in Table I. For the centrality dependent  $v_2(\eta)$  analysis the data samples were subdivided into three centrality classes shown in Table I. The top 3% of the cross-section, where the flow signal is smallest, was omitted in order to reduce the resulting statistical and systematic errors on the most central bin. Differences in the average number of participants between the two methods, for the same fraction of the Au+Au cross-section, occur because the track-based method is track weighted whereas the hit-based method is event weighted. This results in slightly higher  $\langle N_{\text{part}} \rangle$  values for the track-based method, which are insignificant given the systematic error in  $\langle N_{\text{part}} \rangle$  of approximately 4 participants. For both methods the resulting centrality classes are unbiased. The summary of the number of events used is also given in Table I.

Monte Carlo (MC) simulations of the detector performance based on the HIJING [17] event generator and GEANT 3.21 [18] simulation package were used for systematic error studies.

The hit-based method used for the 200 GeV data analysis is exactly the same as described in [11]. Figure 1 shows the minimum-bias result at 200 GeV using this method. The data show a steady decrease in  $v_2$  with increasing  $\eta$  similar to that seen at the lower energy of  $\sqrt{s_{\text{NN}}} = 130$  GeV (also shown in the figure for comparison). No significant difference in shape or magnitude is seen within the systematic errors. The ratio of  $v_2$  at  $\sqrt{s_{\text{NN}}} = 200$  GeV compared to 130 GeV, averaged over all  $\eta$ , is 1.04 ± 0.03 (stat.) ± 0.04 (syst.).

The track-based method correlates the azimuthal angle of tracks that traverse the spectrometer,  $\eta_{\text{trk}}$ , with the

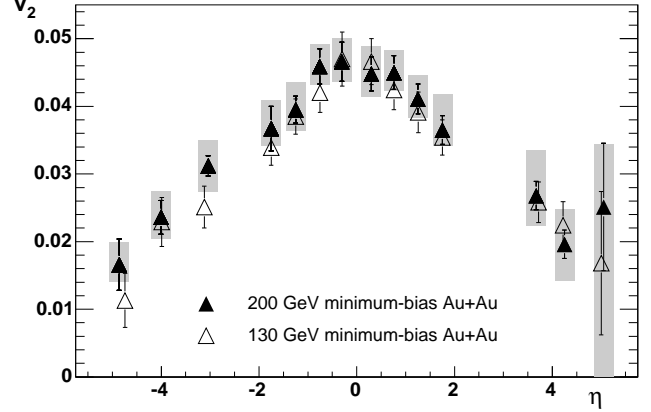


FIG. 1: Elliptic flow as a function of pseudorapidity ( $v_2(\eta)$ ) for charged hadrons in minimum-bias collisions at  $\sqrt{s_{\text{NN}}} = 130$  GeV (open triangles) [11] and 200 GeV (closed triangles). Systematic errors (90% C.L.) are shown as grey boxes only for the 200 GeV data.

event plane as measured in the octagon,  $\eta_{\text{ep}}$ , event by event. The method used is based upon the scheme described by Poskanzer and Voloshin [19], where the strength of the flow is given by the  $n^{\text{th}}$  Fourier coefficient of the particle azimuthal angle distribution

$$\frac{dN}{d(\eta_{\text{trk}} - \eta_{\text{ep}})} \propto 1 + \sum_n 2v_n \cos[n(\eta_{\text{trk}} - \eta_{\text{ep}})]; \quad (1)$$

In this analysis only the  $n = 2$  component is studied and the true reaction plane,  $\eta_{\text{ep}}$ , is approximated by the event plane  $\eta_{\text{ep}}$ .

The use of tracking requires that events with vertices near the nominal vertex range ( 8 cm  $< v_z <$  10 cm) be used to ensure maximum track acceptance in the spectrometer. Because of azimuthal holes in the OCT detector around mid-rapidity, only the parts of the OCT detector with complete azimuthal acceptance are used to determine the reaction plane. Two sub-events, symmetric in and of equal charged particle multiplicity, are used in order to determine the event plane resolution. The extent of these symmetric sub-events is chosen to maximize their acceptance and reaction plane resolution. Consequently, the sub-event sizes become vertex dependent, resulting in a resolution correction that is both centrality and vertex dependent. The resulting sub-event ranges lie between  $2.05 < |\eta| < 3.2$ , and are widely separated, thus greatly reducing the effects of any short range non-flow correlations. The event plane is determined using

$$\eta_{\text{ep}} = \frac{1}{2} \tan^{-1} \frac{\sum_i w_i \sin(2\phi_i)}{\sum_i w_i \cos(2\phi_i)}; \quad (2)$$

where  $\phi_i$  is the  $i^{\text{th}}$  hit's measured angle, and the sums run over all hits in both sub-events. The sub-events are combined for the event plane determination in order to maximize its resolution. Vertex dependent corrections,

Centrality	Hit-based				Track-based			
	% Au+Au	$\langle N_{\text{part}} \rangle$	Number Events	% Au+Au	$\langle N_{\text{part}} \rangle$	Number Events		
minimum-bias	{	205	34,727	0	50	236	5,050,778	
central	3 15	288	11,221	3 15	294	1,439,923		
mid-central	15 25	199	7,550	15 25	202	1,230,394		
peripheral	25 50	111	10,127	25 50	115	3,087,599		

TABLE I: Characteristics of the event samples used in the two flow analyses of 200 GeV Au+Au collisions. For the hit-based minimum-bias event sample, all of the triggered cross-section was used with biases as discussed in the text. The systematic error in  $\langle N_{\text{part}} \rangle$  is approximately 4 participants.

some determined on an event-by-event basis, are used as weights ( $w_i$ ) [11] in order to remove acceptance and occupancy biases. The resulting distributions of event plane angles are found to be at within 2%.

To determine the  $v_2$  coefficient, the measured  $\frac{dN}{d(\text{track}_2)}$  distribution is divided by a mixed event distribution in order to remove detector related effects, such as non-uniformities in the azimuthal acceptance of the spectrometer:

$$\frac{dN}{d\text{measured}} = \frac{dN}{d\text{mixed}} \cdot \frac{1 + 2 \frac{v_2}{C_{\text{res}}} \cos(2\phi)}{C_{\text{res}}} \quad (3)$$

where  $\phi$  denotes track  $\phi_2$  and  $C_{\text{res}}$  is the event plane resolution correction. The  $\frac{dN}{d\text{mixed}}$  distribution, with zero flow, is constructed using an event mixing technique, where the  $\text{track}_2$  of tracks in one event are subtracted from the  $\phi_2$  of another event.

Normalized distributions,  $\frac{dN}{d\text{measured}} = \frac{dN}{d\text{mixed}}$ , and  $C_{\text{res}}$ , are determined as a function of vertex position and for the centrality bins (5% cross-section per bin) since the event mixing technique requires similarity of the class of events examined. The centrality bin and vertex dependent event plane resolution correction  $C_{\text{res}}(\text{centrality}; v_2)$  are determined using the sub-event technique [19] as

$$C_{\text{res}}(\text{centrality}; v_2) = \frac{1}{p_T \frac{2}{2} \cos 2 \frac{<0>}{2} \frac{>0}{2}} \quad (4)$$

where  $\phi_2^{<0>}$  and  $\phi_2^{>0}$  are the event planes from each sub-event. The  $\frac{1}{2}$  factor converts the single sub-event resolution correction into a combined sub-event resolution correction. The factor accounts for the fact that Eq. 4 with  $\phi_2 = 1$  poorly approximates the event plane resolution correction when the correction itself is small. Its exact form is given in Refs. [19] and [20]. For the resolution measured in this data set its values ranged between 1 and 0.95.

After averaging Eq. 3 over vertex positions and centralities falling into each broad centrality class defined in Table I, the  $v_2$  coefficient is extracted from the fit to an even-harmonic series (1) [23]. It should be noted that the resulting  $v_2$  is a track weighted result over the broad centrality classes since limited statistics precluded the

$v_2$  from being determined for each centrality bin and then event weighted. For further details on this technique see [20].

Extensive MC simulations have shown that the magnitude and shape of the flow signal are correctly reproduced by this method. No further corrections to the measured  $v_2$  coefficient are necessary, such as potential corrections due to the density of particles or suppression corrections due to backgrounds, as required in the hit-based method.

In addition to the sources of systematic errors considered for the hit-based analysis [11], other studies were performed for the track-based method. These include analysis of the effects related to tracking such as varying cuts on the distance of closest approach of tracks to the collision vertex, differences between results obtained from the two spectrometer arms, momentum resolution and dependence on the bending direction. Additionally, contributions due to the vertex dependency of the resolution corrections, different beam orbit conditions and errors of the parameters were also accounted for.

Figure 2 shows the centrality dependence of the  $v_2$  determined using the track-based method with the straight line tracks. A pseudorapidity range of  $0 < |\eta| < 1$  is chosen so that a direct comparison can be made with the same result using the hit-based technique. A remarkable agreement is seen between the two techniques over the full range of centrality, supporting the validity of the two independent techniques. The curve in Figure 2 shows a hydrodynamic calculation for Au+Au collisions at  $\sqrt{s_{\text{NN}}} = 200$  GeV [21]. As seen for Au+Au collisions at 130 GeV [2], the 200 GeV results at mid-rapidity for central to semi-central collisions are consistent with expectations from hydrodynamic models. The open triangles in Figure 2 show the results for Au+Au collisions at 130 GeV. Compared to the measured  $v_2$  at 200 GeV, we see within the errors no significant change in either the shape or magnitude of  $v_2$  at mid-rapidity as a function of centrality.

Using tracks that traverse the full field region of the spectrometer, the transverse momentum dependence of the flow strength  $v_2(p_T)$  can be measured. This is shown in Figure 3 for the top 0–50% centrality for tracks averaged over the range  $0 < |\eta| < 1.5$ . The curve shows the prediction of a hydrodynamic model [21]. As previously observed [2] the  $v_2$  rises as  $p_T$  increases and at  $p_T$  above 1.5 GeV/c tends to attenuate well below the hydrodynamic curve.

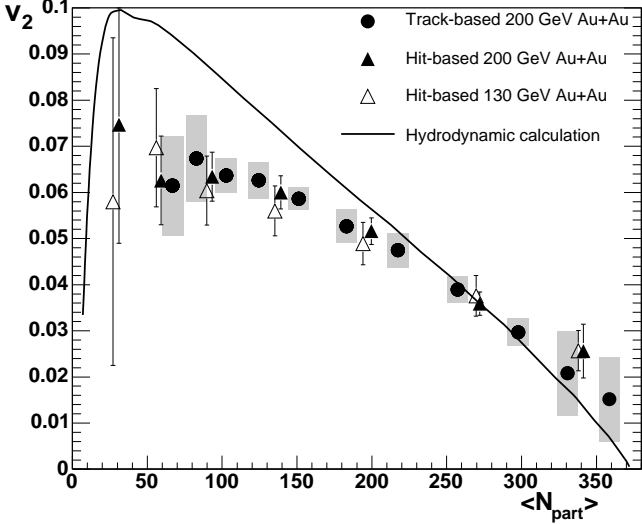


FIG. 2: Elliptic flow ( $v_2 (j < 1)$ ) as a function of  $\langle N_{\text{parti}} \rangle$  determined by the track-based method (closed circles) and hit-based method (closed triangles) for Au+Au collisions at 200 GeV. The open triangles are the  $v_2 (j < 1)$  as a function of  $\langle N_{\text{parti}} \rangle$  results from Au+Au collisions at 130 GeV. The line shows a calculation from hydrodynamics [21] at  $\sqrt{s_{\text{NN}}} = 200$  GeV. The grey boxes show systematic uncertainties for the 200 GeV results from the track-based method.

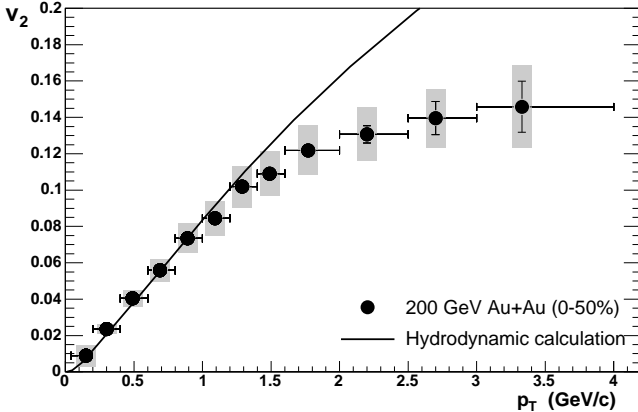


FIG. 3: Elliptic flow as a function of transverse momentum ( $v_2 (p_T)$ ) for charged hadrons with  $0 < < 1.5$  for the most central 50% of the 200 GeV Au+Au collision cross-section. The grey boxes represent the systematic error. The data points are located at the average  $p_T$  position within a  $p_T$  bin whose size is given by the horizontal error bars. The curve shows a calculation from hydrodynamics [21].

It is expected that determining the reaction plane in sub-events that are at different pseudorapidities from those where the  $v_2$  is measured, as in these analyses, should significantly reduce the contribution of non-flow effects to the measured  $v_2$ . This is especially relevant to the non-flow contributions from short range correlations. Comparisons of the  $v_2 (p_T)$  result to the reaction plane and cumulant methods results from reference [5],

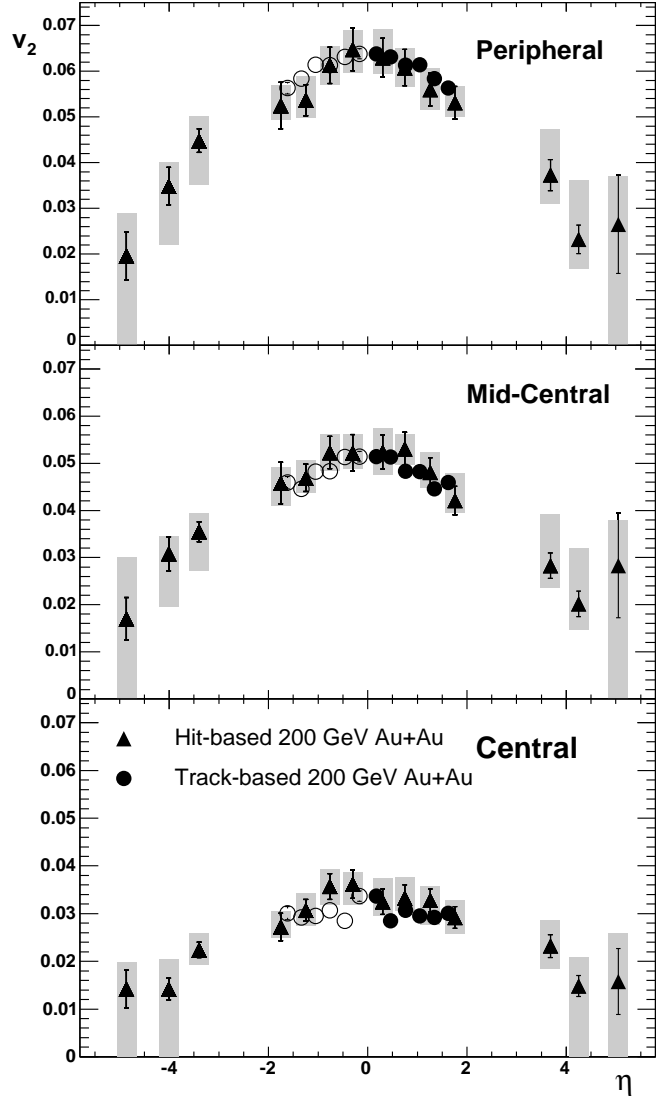


FIG. 4: Elliptic flow as a function of pseudorapidity ( $v_2 (\eta)$ ) for charged hadrons from 200 GeV Au+Au collisions for the three different centrality classes described in the text, ranging from peripheral to central (25–50%, 15–25%, 3–15%) from top to bottom. The triangles are the results from the hit-based method, and the circles are from the track-based method. The open circles are the track-based results reflected about mid-rapidity. Statistical errors are shown as the error bars, and systematic errors for the hit-based method are shown as shaded boxes around each data point.

averaged over a similar centrality range, show that our result is most consistent with the one obtained with the four particle cumulant method [22], suggesting that our track-based methodology is indeed largely immune to non-flow effects over the range  $j < 1.5$ .

Figure 4 shows  $v_2 (\eta)$  for three centrality classes as defined in Table I. The results from the hit-based and track-based methods are overlayed. Excellent agreement is seen across all of the centrality classes over the range of overlap. The good agreement between the two methods

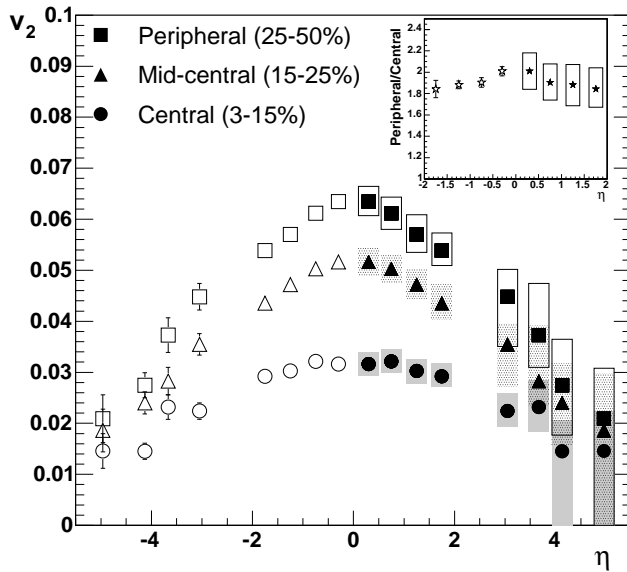


FIG. 5: Elliptic flow as a function of pseudorapidity ( $v_2(\eta)$ ) from 200 GeV Au+Au collisions for the three centrality bins (3–15% circles, 15–25% triangles, 25–50% squares). The data for  $\eta > 0$  is determined by re-jecting the hit-based results about mid-rapidity and then combining them with the track-based results and shown with the systematic errors alone. The same data are re-jected around  $\eta = 0$  and shown as open symbols with statistical errors only. The insert shows the ratio of the peripheral to central combined results where the two methods overlap, with only statistical errors shown for  $\eta < 0$  and only systematic errors shown for  $\eta > 0$ .

ods suggests that our hit-based method is also largely unaffected by non-flow effects around mid-rapidity.

To examine how the shape of the distribution changes with centrality, the results of the hit-based method and track-based methods are combined. Although obtained in the same experiment, the measurements should effectively be considered independent of each other due to the very different methods and elements of the PHOBOS detector that are used. Hence the results for each method are combined with the reasonable assumption that the errors are uncorrelated. The combined results are obtained by first combining the hit-based results that are an equal distance away from mid-rapidity together. The two highest  $j$  points are combined, the points at  $j = 3.05$  and  $j = 3.67$  are just re-jected

due to the lack of symmetry of these points around  $\eta = 0$ . These hit-based results are then combined with the track-based results with similar binning. The statistical and systematic errors are treated separately in the combination. The resulting combined data are shown in Figure 5. To be able to show the statistical and systematic errors more clearly, the negative section shows the combined points with their statistical errors only. The positive section depicts the combined points with their systematic errors only. The pseudorapidity dependence of  $v_2$  for the 3 centrality bins is similar to that observed in Fig. 1 for minimum-bias data. For peripheral collisions,  $v_2$  is clearly already non-zero at over the range  $2 < |\eta| < 2$ . The overall shape of  $v_2(\eta)$  is not strongly centrality dependent within the uncertainties, appearing to differ only by a scale factor. This is illustrated in the insert of Fig. 5, which shows that the ratio of the peripheral to central data around mid-rapidity is approximately constant. However, it should be noted that the central data around mid-rapidity is also consistent with a flat distribution, given the statistical and systematic uncertainties.

In summary we have measured the centrality dependence of  $v_2(\eta)$  in Au+Au collisions at  $\sqrt{s_{NN}} = 200$  GeV. Excellent agreement with the track-based method further validates the use of the hit-based method. This method allowed for the study of the  $v_2(\eta)$  dependence over the large range of  $\eta$  covered by the PHOBOS single-layer silicon detectors. The 200 GeV results clearly show that  $v_2$  decreases with increasing  $|\eta|$  as seen for the 130 GeV Au+Au collisions. From comparisons of the  $v_2(p_T)$  results with four-particle cumulant results we conclude that our flow measurements are largely immune to non-flow effects, over the range  $|\eta| < 1.5$ .

The predominant features of the  $v_2(\eta)$  distribution do not change significantly as a function of centrality from  $N_{part} = 290$  to  $N_{part} = 110$ . The flow still falls off as one moves away from mid-rapidity. It is hoped that this data can be used to more fully understand the strong dependence of the  $v_2$  flow component.

This work was partially supported by U.S. DOE grants DE-AC02-98CH10886, DE-FG02-93ER40802, DE-FG02-94ER40818, DE-FG02-94ER40865, DE-FG02-99ER41099, and W-31-109-ENG-38, US NSF grants 9603486, 9722606 and 0072204, Polish KBN grant 2-P03B-10323, and NSC of Taiwan contract NSC 89-2112-M-008-024.

[1] B. B. Back et al., Phys. Rev. Lett. 91, 072302 (2003);  
 J. Adams et al., Phys. Rev. Lett. 91, 072304 (2003);  
 S. S. Adler et al., Phys. Rev. Lett. 91, 072303 (2003);  
 I. Arsene et al., Phys. Rev. Lett. 91, 072305 (2003).  
 [2] K. H. Ackermann et al., Phys. Rev. Lett. 86, 402 (2001).  
 [3] C. Adler et al., Phys. Rev. Lett. 87, 182301 (2001).  
 [4] C. Adler et al., Phys. Rev. Lett. 89, 132301 (2002).

[5] C. Adler et al., Phys. Rev. C 66, 034904 (2002).  
 [6] C. Adler et al., Phys. Rev. Lett. 90, 032301 (2003).  
 [7] C. Adler et al., Phys. Rev. Lett. 92, 052302 (2004).  
 [8] C. Adler et al., Phys. Rev. Lett. 92, 062301 (2004).  
 [9] K. Adcox et al., Phys. Rev. Lett. 89, 212301 (2002).  
 [10] S. S. Adler et al., Phys. Rev. Lett. 91, 182301 (2003).  
 [11] B. B. Back et al., Phys. Rev. Lett. 89, 222301 (2002).

- [12] B. B. Back et al, submitted to Phys. Rev. Lett., arXiv:nucl-ex/0406021.
- [13] B. B. Back et al, Nucl. Inst. Meth. A 499, 603 (2003).
- [14] B. B. Back et al, Phys. Lett. B 578, 297 (2004).
- [15] B. B. Back et al, Phys. Rev. Lett. 85, 3100 (2000).
- [16] B. B. Back et al, Phys. Rev. C 65, 061901 (2002).
- [17] M. Gyulassy and X. N. Wang, Comput. Phys. Commun. 83, 307 (1994). HIJING v1.35 used.
- [18] R. Brun, F. B. Ruyant, M. M. Fair, A. C. M. Cherson and P. Zanarini, Geant3. Technical Report CERN-DD/EE/84-1, CERN, 1984.
- [19] A. M. Poskanzer and S. A. Voloshin, Phys. Rev. C 58, 1671 (1998).
- [20] C. M. Vale, Ph. D. thesis, Massachusetts Institute of Technology (2004).
- [21] P. F. Kolb, P. Huovinen, U. W. Heinz and H. Heiselberg Phys. Lett. 500, 232 (2001); P. Huovinen, Private Communication.
- [22] PHOBOS Collaboration, M. B. Tsatsas et al, nucl-ex/0403025, to appear in the Proceedings of the Seventeenth International Conference on Ultra-Relativistic Nucleus-Nucleus Collisions, Oakland, CA, January 2004.
- [23] Including orders higher than  $n = 2$  in the  $t$  did not effect the extracted  $v_2$ .